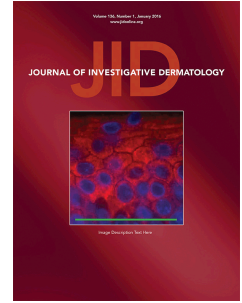# Journal Pre-proof

Molecular signature of pruriceptive MrgprA3^{+} neurons

Yanyan Xing, Junyu Chen, Henry Hilley, Haley Steele, Jingjing Yang, Liang Han

Please cite this article as: Xing Y, Chen J, Hilley H, Steele H, Yang J, Han L, Molecular signature of pruriceptive MrgprA3^{+} neurons, *The Journal of Investigative Dermatology* (2020), doi: https://doi.org/10.1016/j.jid.2020.03.935.

This is a PDF file of an article that has undergone enhancements after acceptance, such as the addition of a cover page and metadata, and formatting for readability, but it is not yet the definitive version of record. This version will undergo additional copyediting, typesetting and review before it is published in its final form, but we are providing this version to give early visibility of the article. Please note that, during the production process, errors may be discovered which could affect the content, and all legal disclaimers that apply to the journal pertain.

Molecular signature of pruriceptive MrgprA3+ neurons

Yanyan Xing[1], Junyu Chen[2], Henry Hilley[1], Haley Steele[1], Jingjing Yang[2], Liang Han[1]*

1 School of Biological Sciences, Georgia Institute of Technology, Atlanta, GA 30332

2 Department of Human Genetics, Emory University School of Medicine, Atlanta, GA 30322

*Corresponding author: Liang Han, PhD, School of Biological Sciences, Georgia Institute of

Technology, Atlanta, GA 30332, USA. Email: liang.han@biology.gatech.edu

ABSTRACT

Itch, initiated by the activation of sensory neurons, is frequently associated with dermatological diseases. MrgprA3$^+$ sensory neurons have been identified as one of the major itch-sensing neuronal populations. Mounting evidence has demonstrated that peripheral pathological conditions induce physiological regulations of sensory neurons, which is critical for the maintenance of chronic itch sensation. However, the underlying molecular mechanisms are not clear. Here we performed RNA sequencing of genetically labeled MrgprA3$^+$ neurons under both naïve and allergic contact dermatitis conditions. Our results revealed the unique molecular signature of itch-sensing neurons and the distinct transcriptional profile changes that result in response to dermatitis. We found enrichment of nine Mrgpr family members and two histamine receptors in MrgprA3$^+$ neurons, suggesting that MrgprA3$^+$ neurons are a direct neuronal target for histamine and Mrgprs agonists. In addition, Ptpn6 and Pcdh12 were identified as highly selective markers of MrgprA3$^+$ neurons. We also discovered that MrgprA3$^+$ neurons respond to skin dermatitis in a way that is unique from other sensory neurons by regulating a combination of transcriptional factors, ion channels, and key molecules involved in synaptic transmission. These results significantly increase our knowledge of itch transmission and uncover potential targets for combating itch.

INTRODUCTION

Chronic itch is a devastating symptom frequently associated with dermatological diseases such as atopic dermatitis, psoriasis, and lichen planus (Yosipovitch and Bernhard, 2013). Itch sensation is initiated by the activation of sensory neurons whose cell bodies reside in the dorsal root ganglion (DRG) or trigeminal ganglion (TG). Skin innervating sensory neurons project their peripheral and central axons to the skin and spinal cord respectively, providing a bridge for information flow from the peripheral skin to the central nervous system. Cutaneous stimuli or insults in the inflamed skin, such as pruritogens, are transduced into neuronal activities in the skin nerves to activate itch neural circuits and convey the signals to the brain (Ikoma et al., 2006).

Three pruriceptive sensory neuron subtypes have been identified by both functional studies and single-cell RNA-seq analysis and named NP1-3, each of which expresses distinct itch receptor combinations (Chiu et al., 2014, Hu et al., 2016, Kupari et al., 2019, Li et al., 2016, Sharma et al., 2020, Usoskin et al., 2015, Zeisel et al., 2018). NP1 neurons are classified by the expression of MrgprD (Liu et al., 2012), whereas NP2 neurons are classified by the expression of MrgprA3 and MrgprC11 (Han et al., 2013, Liu et al., 2009). NP3 neurons express the most itch receptors, including two co-receptors for IL-31 (Il31ra and osmr), Cysltr2 (cysteinyl leukotriene receptor 2), Htr1f (5-Hydroxytryptamine Receptor 1F) and S1pr1 (sphingosine-1-phosphate receptor 1) (Huang et al., 2018, Mishra and Hoon, 2013, Solinski et al., 2019, Storan et al., 2015, Usoskin et al., 2015).

Peripheral pathological conditions can profoundly change the physiological properties of the innervating sensory neurons and modulate the communication of sensory neurons with second-order spinal neurons by utilizing both transcriptional and translational modifications (Basbaum et al., 2009, Piomelli and Sasso, 2014, Waxman and Zamponi, 2014). Indeed, our recent studies

demonstrated that NP2 MrgprA3$^+$ neurons exhibit elevated itch receptor expression and hyperinnervation in the skin in a mouse dry skin model (Zhu et al., 2017) and enhanced excitability and spontaneous activities in a contact dermatitis model (Qu et al., 2014). However, the molecular mechanisms underlying those changes are not clear. Our study presents extensive transcriptional profiling of pruriceptive MrgprA3$^+$ and demonstrate distinct transcriptional profile changes in both MrgprA3$^+$ and MrgprA3$^-$ neurons following allergic contact dermatitis.

RESULTS:

MrgprA3$^+$ neurons are a distinct subpopulation of DRG sensory neurons

In our previous study we generated a *MrgprA3$^{GFP-Cre}$* line in which the expression of GFP-Cre is controlled by the *MrgprA3* promoter (Han et al., 2013). We treated the lower back skin of *MrgprA3$^{GFP-Cre}$* mice to induce allergic contact dermatitis (ACD). We selected the lower back skin to minimize possible scratching-induced skin injury since mice are not able to scratch their lower back skin effectively. The treatment induced parakeratosis, dense inflammatory cell infiltration in the skin (Figure 1A), and spontaneous scratching behavior (Figure 1B). Thoracic and lumbar DRGs (T11-L6) innervating the treated skin area were isolated after treatment and enzymatically dissociated. MrgprA3$^+$ neurons and MrgprA3$^-$ neurons were FACS purified based on GFP fluorescence, and the total RNA was extracted for RNA-seq analysis. Principal Components Analysis (PCA) showed clear segregation of MrgprA3$^+$ and MrgprA3$^-$ neurons, both before and after the ACD treatment (Figure 1C), demonstrating that MrgprA3$^+$ neurons are a distinct subpopulation of DRG sensory neurons. To quantitatively evaluated the difference in the transcriptome profiles of different groups, we used the support vector machine (svm)-based classification model to classify control and ACD treatment samples (Cortes and Vapnik, 1995). The area under the ROC (receiver operating characteristic) curve (Fawcett, 2006) is clearly

4

higher for the MrgprA3$^+$ neuron samples (Figure 1D), suggesting that the MrgprA3$^+$ neurons

exhibited larger transcriptome profile change compare to the MrgprA3$^-$ neurons after ACD

treatment. This data is consistent with the key role MrgprA3$^+$ neurons play in mediating ACD

itch.

Transcriptional profile of MrgprA3$^+$ neurons

We first compared the data from MrgprA3$^+$ and MrgprA3$^-$ populations in the control group. In

total 1,845 DEGs, including 584 upregulated genes and 1,261 downregulated genes, were

identified in MrgprA3$^+$ neurons (Supplementary Table 1). Significant GO Biological Process

terms of the genes enriched in MrgprA3$^+$ neurons include itch (Custom GO Term), membrane

hyperpolarization, and response to ATP, consistent with MrgprA3$^+$ neurons function as itch-

sensing neurons (Figure 1E). Conversely, GO terms associated with genes enriched in MrgprA3$^-$

neurons include pain, thermal sensation, mechanical sensation, and locomotion, which is

unsurprising because MrgprA3$^-$ neurons include pain sensors, touch sensors, and proprioceptors

(Figure 1F). GO terms such as neurogenesis, neuron differentiation, and ion transport are

associated with genes enriched in both groups, suggesting that the two neuronal populations

engage different gene sets to perform the same biological process. Similar results were also

demonstrated by the GO Molecular Function analysis (transmembrane transporter activity and

cation channel activity). Many GO categories associated with MrgprA3$^+$ neurons are related to

ion channels in GO-MF, suggesting that MrgprA3$^+$ neurons utilize distinct groups of ion

channels to perform neuronal functions.

We next examined the gene expression pattern of known genes that are important for sensory

neuron functions. The first group we analyzed were Mrgpr (mas-related G protein-coupled

receptor) family members (Meixiong and Dong, 2017) (Figure 2A). Consistent with previous

studies from our group and others, MrgprB4, MrgprC11, and MrgprA1 are enriched in

MrgprA3+ neurons (Han et al., 2013, Li et al., 2016, Lou et al., 2015, Meixiong et al., 2019a).

Five other Mrgprs with unknown functions including MrgprA2b, MrgprA4, MrgprA7, MrgprA8,

and MrgprB5 are also highly enriched in MrgprA3+ neurons. It is interesting to see nine

members of the same family enriched in MrgprA3+ neurons, which only constitute 8% of the

DRG sensory neurons.

We then analyzed 19 known genes that play an important role in itch sensation (Figure 2B). Two

histamine receptors (Hrh1 and Hrh2) and Plcβ3, an isozyme mediating histamine-induced

sensory neuron activation, are enriched in MrgprA3+ neurons (Han and Dong, 2014, Han et al.,

2006). This is confirmed by the triple *in situ* hybridization detecting histamine receptors (Hrh1

and Hrh2), Plcβ3, and MrgprA3 (Figure 4A-B). We found that ~14% of DRG neurons express

both Hrh1 and Plcβ3, suggesting that they are histamine-sensing neurons. The majority of

MrgprA3+ neurons (82.9%) express both Hrh1 and Plcβ3. Similar results were observed for Hrh2.

We did not observe the expression of Hrh4 in DRG sensory neurons. Neuromedian B (Nmb), a

neuropeptide required for scratching behaviors induced by histamine, compound 48/80, and 5-

HT (Wan et al., 2017), is also enriched in MrgprA3+ neurons. The enrichment of these genes and

Mrgprs suggests that MrgprA3+ neurons are important direct mediators of the Mrgprs agonists

and histamine-induced itch.

As MrgprA3- neurons include NP1 and NP3 populations (Usoskin et al., 2015), they are

similarly enriched for many itch receptors and itch-related molecules including Nppb

(Natriuretic Peptide B) and Sst (somatostatin). Both co-receptors for IL-31 (Il31ra and osmr) are

highly expressed in both MrgprA3+ and MrgprA3- neurons, although MrgprA3- neurons are

more enriched for Il31ra, suggesting that MrgprA3+ neurons are part of the neuronal population

mediating Il-31-induced itch. Lpar1 and Lpar3 (Lysophosphatidic acid receptors) are downregulated in MrgprA3$^+$ neurons (Kremer et al., 2010). The expression of both endothelin receptors and endothelin converting enzyme 1 (Ece1) (Kido-Nakahara et al., 2014) is relatively higher in MrgprA3$^-$ population. Htr7 (5-Hydroxytryptamine Receptor 7) (Morita et al., 2015) is preferentially expressed in MrgprA3$^-$ neurons.

We next examined the expression patterns of several families that are key players in nociception, which include TRP channels, purinergic receptors, prostaglandin receptors, and acid-sensing ion channels (Basbaum et al., 2009) (Figure 2C-D). The only TRP channel enriched in MrgprA3$^+$ neurons is TRPC3, whose function in itch sensation is not yet clear (Figure 2C). Three other genes are observed to be specifically enriched in MrgprA3$^+$ neurons including P2rx2 (ionotropic purinergic receptor 2), P2ry2 (metabotropic purinergic receptor 2), and Ptger4 (prostaglandin E receptor 4, or EP4). The enrichments of P2rx2 and P2ry2 raise the question if ATP plays a role in itch induction, which has not been intensively investigated yet. Previous studies have shown an increased level of prostaglandin E2, an agonist for EP4, in the skin of patients with atopic dermatitis (Fogh et al., 1989). Consistently, blockade of PGE2 signaling reduced spontaneous scratching behavior in a mouse model of dermatitis (Emrick et al., 2018). Our analysis suggests that PGE2 might activate MrgprA3$^+$ neurons via the activation of EP4.

Many markers for non-pruriceptive neurons are downregulated in MrgprA3$^+$ neurons (Figure 2F) including markers for large-diameter neurons (vGlut1, Ldhb, Cavna1h, Spp1, and Fam19a1), markers for proprioceptors (Pvalb), and marker for C-low-threshold mechanoreceptors (TH and vGlut3) (Usoskin et al., 2015). Nefm (neurofilament medium chain) and Nefh (neurofilament heavy chain) are enriched in MrgprA3$^-$ neurons. By contrast, Ina, an internexin neuronal intermediate filament, is enriched in MrgprA3$^+$ neurons. Expression of neurotrophin receptors

7

has long been one of the criteria to classify somatosensory neurons (Lallemend and Ernfors, 2012). MrgprA3^{+} neurons are enriched for Gfra1 (GDNF receptor alpha 1) and Ntrk1 (TrkA, neurotrophic receptor tyrosine kinase 1). Interestingly, we also observed the enrichment of Runx2 (runt related transcription factor 2), the only Runx family member that has not been linked to somatosensory neurons differentiation and function, in MrgprA3^{+} neurons (Figure 2E).

Similar to the previous single-cell RNA-seq analysis, we found MrgprA3^{+} neurons are enriched for Nmb (neuromedin B), CGRP (Calca, and Calcb, calcitonin/calcitonin-related polypeptide, alpha and beta), and Agrp (Agouti-related peptide). In addition, we found that MrgprA3^{+} neurons are enriched for Pcsk2 (Proprotein Convertase Subtilisin/Kexin Type 2), and Pcsk1n (Proprotein Convertase Subtilisin/Kexin Type 1 Inhibitor), both of which are involved in the processing of neuropeptide and have never been linked to sensory neuron function (Figure 2G).

MrgprA3^{+} neurons employ unique combinations of ion channels to maintain the resting membrane potential and initiate the neuronal firing. For sodium channels (Figure 3A), Nav1.9 (Scn11a) is enriched in MrgprA3^{+} neurons, which is in line with its known role in itch sensation (Salvatierra et al., 2018). The other two enriched members in MrgprA3^{+} neurons are β subunits of voltage-gated sodium channels Scn2b and Scn3b. Cacng2 is the only enriched voltage-gated calcium channel in the MrgprA3^{+} neurons (Figure 3B). Ttyh2 (Drosophila tweety homolog 2), a calcium-activated chloride channel (Suzuki, 2006), is highly enriched in MrgprA3^{+} neurons (Figure 3C). We observed seven potassium channels enriched in MrgprA3^{+} neurons with Kcnk18 as the only enriched leaky potassium channel (TRESK, potassium channel, subfamily K, member 18) (Figure 3D) (Sano et al., 2003).

To validate the enriched transcripts *in vivo*, we chose two genes (Ptpn6 and Pcdh12) identified to be highly enriched in MrgprA3^{+} neurons for RNAscope *in situ* hybridization analysis (Figure 4).

8

83.3% (80/96) of Ptpn6$^+$ (Protein Tyrosine Phosphatase Non-Receptor Type 6) neurons are expressing MrgprA3 (Figure 4A) and the majority of Pcdh12$^+$ (protocadherin 12) neurons (69.9%, 93/133) coexpress MrgprA3. These results show that the enriched genes identified by our RNA-seq analysis also exist *in vivo*.

Transcriptional profile of MrgprA3$^+$ neurons was changed by atopic contact dermatitis

ACD treatment significantly changed the expression profile of both MrgprA3$^+$ neurons and MrgprA3$^-$ neurons, demonstrating the common neuro-immuno crosstalk between inflamed skin and innervating sensory neurons. We have identified 408 upregulated genes and 425 downregulated genes in MrgprA3$^+$ neurons (Figure 5A, Supplementary Table 2). Similarly, 292 upregulated genes and 420 downregulated genes were identified in MrgprA3$^-$ neurons (Figure 5A, Supplementary Table 3). Inflamed skin caused significant damage to all of the innervating sensory neurons, as demonstrated by the enrichment of GO terms such as programmed cell death and cellular response to stress associated with both neuron types. However, the genes affected in the two neuronal populations are largely non-overlapping (Figure 5A), which indicates that MrgprA3$^+$ neurons respond to the dermatitis condition in a very different way from other sensory neuron subtypes. Indeed, unique GO terms are identified to be associated with the two neuronal populations (Figure 5B).

A small percentage of affected genes (Figure 5A, Supplementary Table 4) were changed in both neuronal populations. Among them, we identified several interesting genes including those related to inflammatory responses such as Il17ra (interleukin 17 receptor A), Tnfrsf1a (tumor necrosis factor receptor superfamily, member 1a), and Ptgfr (prostaglandin F receptor); those related to neuronal function such as Syt2 (synaptotagmin II), Syt7 (synaptotagmin II), and Slc12a2 (Sodium/Potassium/Chloride Transporter, Solute Carrier Family 12, Member 2); and

those related to intracellular signaling transduction in sensory neurons such as Pla2r1 (phospholipase A2 receptor 1) and Dgkz (diacylglycerol kinase zeta).

Distinct sets of transcription factors were identified within the two neuronal populations (Figure 6A), the majority of which lack known sensory neuron function. Etv5, an essential molecule regulating sensory neuron differentiation and axonal growth during development (Fontanet et al., 2013), is upregulated in MrgprA3+ neurons. Six4, a transcriptional factor required for the survival of sensory neurons, is downregulated in MrgprA3+ neurons (Konishi et al., 2006, Moody and LaMantia, 2015, Yajima et al., 2014). Runx1 and Prdm12, both of which are required for nociceptor specification, are downregulated in MrgprA3- neurons (Bartesaghi et al., 2019, Chen et al., 2006, Desiderio et al., 2019, Kramer et al., 2006, Liu et al., 2008).

We then focused our analysis on the genes related to sensory neuron function (Figure 6B). Both MrgprA3+ and MrgprA3- neurons showed distinct gene change pattern after ACD treatment. Three itch receptors (Hrh2, Il31ra, and Lpar3) were changed in MrgprA3- neurons, while we did not observe any significant change of itch receptors in MrgprA3+ neurons. ASIC3 (acid-sensing ion channel 3), P2rx5 (ionotropic purinergic receptor 5), and Ptges (prostaglandin E synthase) were changed in MrgprA3+ neurons, while Bdkrb2 (Bradykinin receptor beta 2), P2rx6 (metabotropic purinergic receptor 6) and Ptges2 (prostaglandin E synthase 2) were changed in MrgprA3- neurons. A TNF receptor (Tnfrsf1a) and several interleukin receptors (Il1r1, Il1ra, and Il17ra) were changed, indicating their involvement in sensory neurons in response to skin inflammation. Interestingly, we observed a significant increase of Ngfr (nerve growth factor receptor, or P75) only in MrgprA3+ neurons, consistent with the role of NGF in promoting chronic itch and sensory nerve sensitization (Ikoma et al., 2006, Mollanazar et al., 2016). Many ion channels have been identified as well, indicating the change of electrophysiological

properties of neurons (Figure 6C). Among them, Cacng5 (calcium channel, voltage-dependent, gamma subunit 5) shows the greatest changes in MrgprA3$^+$ neurons, while Kcne3 (potassium voltage-gated channel, Isk-related subfamily, gene 3) shows the greatest change in MrgprA3$^-$ neurons.

Studies have shown that peripheral insults can lead to changes in the sensory signal transmission to spinal cord neurons and presynaptic regulation by the local spinal circuits or descending fibers. Indeed, we found significant changes in many neurotransmitter receptors (Figure 6D). Among them, Gria2 (GluR2) was increased in both MrgprA3$^+$ and MrgprA3$^-$ neurons. Many genes related to synaptic transmission were also identified (Figure 6E-F) including Syt2 (synaptotagmin II), which was increased in both neuron types, Syt7 (synaptotagmin VII), which was decreased in both neuron types, and Camk2b (Calcium/Calmodulin Dependent Protein Kinase II Beta), which was decreased in MrgprA3$^+$ neurons.

We used real-time RT-PCR to validate the expression changes of several genes (Figure 6F) that represent the different categories we discussed above and are interesting for future investigations. Syt7 and Dgkz were selected since their functions in sensory neurons are unknown and they both showed the same trend of change in both MrgprA3$^+$ and MrgprA3$^-$ neurons in the RNAseq analysis. Syt7 is a calcium sensor regulating synaptic vesicle release and its role in DRG sensory neurons has never been explored (Bacaj et al., 2013, Liu et al., 2014). Dgkz, a member of the diacylglycerol kinase family that regulates intracullar signaling pathway involving lipid messengers diacylglycerol and phosphatidic acid, is highly expressed in sensory neurons with unclear function (Shirai and Saito, 2014). Camk2b and Kcne3 were selected since they showed strongest changes in the list of synaptic-related genes and potassium channels respectively. Runx1 and Il31ra were selected because they showed significant changes only in MrgprA3$^-$

neurons. Il31ra is one of the most studied itch receptors and is enriched in pruriceptive NP3

neurons (Li et al., 2016, Usoskin et al., 2015). Runx1 is a key transcription factor for nociceptor

specification and has an undiscovered role in itch. The investigation of both will help us to

understand the changes induced in MrgprA3$^-$ neurons by the ACD treatment. Interestingly,

results of the real-time PCR analysis of all six genes are consistent with the RNAseq analysis

(Figure 6F).

DISCUSSION

Analogous to the T2Rs bitter receptor family in the gustation system and odorant receptor family

in the olfaction system (Secundo et al., 2014, Yarmolinsky et al., 2009), Mrgpr family contains a

large group of G protein-coupled receptors with different members detecting different

pruritogens. MrgprA1 mediates substance P-induced itch (Azimi et al., 2017). MrgprA3

responds to anti-malaria drug chloroquine (Liu et al., 2009). MrgprC11 mediate Bam8-22,

SLIGRL, cathepsin S, and cysteine protease Der p1-induced itch (Liu et al., 2009, Liu et al.,

2011, Reddy and Lerner, 2017, Reddy et al., 2015), while MrgprD is responsible for β-alanine-

induced itch (Liu et al., 2012). Consistently, two human Mrgpr family member X1 and X4 have

been demonstrated to mediate itch sensation evoked by chloroquine and cholestasis respectively

(Liu et al., 2009, Meixiong et al., 2019b, Yu et al., 2019). In the olfactory system, each olfactory

receptor neuron within the olfactory epithelium only expresses a single odorant receptor. The

identity of odorants is encoded by a combinatorial receptor code with each odorant receptor

responding to multiple odorants and each odorant activating multiple receptors (Secundo et al.,

2014). This strategy allows the olfactory system to distinguish a massive number of odorant

molecules, which is critical for recognizing food, predators, and mates. In contrast, in the

gustation system, it is more important for bitter taste to reveal the safety of potential food than to

12

identify different bitter compounds. Therefore, multiple bitter taste receptors are co-expressed in the same taste receptor cells and stimulate the same neural circuits upon activation (Yarmolinsky et al., 2009). Interestingly, we found that MrgprA3$^+$ neurons are enriched for two histamine receptors and eight other Mrgpr family members including two identified itch receptors MrgprA1 and MrgprC11, and five other members: MrgprB4, MrgprA2b, MrgprA4, MrgprA7, and MrgprA8. These results demonstrate that the somatosensory system employs the same strategy as the gustation system for detecting itch. Multiple itch receptors are highly enriched in MrgprA3$^+$ neurons to ensure the detection of the somatosensory modality of the stimuli (itchy), while the identity of each pruritogen, which is not critical for the safety and survival of the animals, can be ignored. Similarly, the pruriceptive NP3 neurons also express multiple itch receptors including Il31ra, osmr, Cysltr2, Htr1f, and S1pr1. This expression pattern of itch receptors supports the hypothesis that itch sensing is mediated by a labeled line in the peripheral sensory neurons (Han and Dong, 2014).

Our sequencing analysis reveals the expression of unique combinations of GPCRs, neuropeptides, neurotrophic factors, and ion channels in MrgprA3$^+$ neurons. The analysis of many genes is consistent with previous single-cell RNA-seq analysis such as the enrichment of MrgprB4, Rspo1, and Gfra1 in MrgprA3$^+$ neurons and the enrichment of Il31ra, Nppb, Sst, and Lpar3 in MrgprA3$^-$ neurons (Li et al., 2016, Usoskin et al., 2015). Our analysis also discovered several genes that have not previously been identified in MrgprA3$^+$ neurons such as MrgprA4, MrgprA7, Ptpn6, and Pcdh12. Understanding the function of those genes in itch transmission will possibly lead to a better understanding of the basic mechanisms of itch transmission.

Chronic itch is induced by the generation of a high level of endogenous agonists for itch-sensing neurons in pathological conditions. It can be enhanced and maintained by the abnormal function

13

of sensory neurons, as well as changes in the synaptic transmission between sensory neurons and spinal neurons. We did not observe any itch receptor change in MrgprA3$^+$ neurons, suggesting that skin inflammation does not regulate receptor expression to changes neuronal sensitivity. However, we observed a change in the expression of genes in the following categories: transcriptional factors (such as Etv5 and Six4), purinergic receptor (such as P2rx5), ion channels (such as ASIC3 and Cacng5), neurotransmitter receptors (Gria2), and key molecules in synaptic transmission (such as Syt2 and Syt7), all of which may contribute to the generation of chronic itch in dermatitis skin. The change in the TNF receptor (Tnfrsf1a) and interleukin receptors (Il1r1, Il1ra, and Il17ra) also suggest one possible way that the sensory nerves respond to the inflammatory condition in the skin. In MrgprA3$^-$ neurons, we observed the upregulation of three itch receptors Hrh2, Il31ra, and Lpar3 after ACD treatment. Lpar3 and Il31ra are highly expressed in pruriceptive NP1 and NP3 population respectively. These results suggest the involvement of all three types of pruriceptive sensory neurons in mediating ACD itch.

The mechanisms underlying these changes in transcriptional profiles might be distinct for different types of genes. The inflammatory soup in the ACD skin contains molecules secreted by all recruited immune cells and residential skin cells such as keratinocytes, all of which might play a role in controlling the gene expression changes in the innervating sensory neurons. For example, a classical molecule that is upregulated in atopic dermatitis skin is NGF (Dou et al., 2006), a growth factor that can be secreted by keratinocytes (Di Marco et al., 1991) and regulates neuronal survival and nerve sprouting via transcriptional regulation (Ikoma et al., 2006, Patel et al., 2000, Tominaga et al., 2011). Consistently, we have observed the upregulation of Ngfr in MrgprA3$^+$ neurons. Upregulation of IL-31, a cytokine primarily produced by Th2 cells that activates multiple transcriptional factors within neurons, is also observed in atopic dermatitis

skin (Mollanazar et al., 2016). The increased expression of Il31ra in MrgprA3$^-$ neurons suggests the involvement of IL-31 signaling in transcriptional regulation.

In summary, our study reveals the distinct transcriptional profile of pruriceptive MrgprA3$^+$ neurons and unique gene regulation in response to peripheral allergic inflammation. Further functional studies investigating the role of identified genes in chronic itch will provide insights into the basic molecular and cellular mechanisms of itch and help to discover therapeutic targets for relieving itch.

MATERIALS AND METHODS:

Mice and contact dermatitis treatment

All experiments were performed with approval from the Georgia Institute of Technology Animal Use and Care Committee. Mice were housed in the vivarium with a 12-hr-light/dark cycle, and all the behavioral tests were performed from 9 a.m. to 1 p.m. in the light cycle. The housing group was 5 at maximum with food and water *ad libitum*. A mouse model of allergic contact dermatitis was produced as described previously with 2-month old males (25 - 30g) C57BL/6 mice (Zhu et al., 2017). Briefly, on day 1-3, SADBE (squaric acid dibutylester, 25ul, 0.5% in acetone) was applied to the shaved abdomen once a day. On days 8-12, SADBE was applied to the shaved lower back skin to induce dermal inflammation. 5 mice were used in both the SADBE treatment group and the control group. On day 13, animals were first recorded for 60 min to examine scratching behaviors and then thoracic and lumbar DRGs (T11-L6, totally 16 DRGs) innervating the treated skin area from every animal were isolated for FACS. We use T12 DRG as the landmark to identify the axial level of all collected DRGs. T12 DRG is the ganglion immediately caudal to the last rib of the animal. Treated skin was also collected for histological analysis at the same time. Mice in the control group were handled exactly the same way as the mice in SADBE group by the experimenters, but were only treated with acetone which is the solvent for SADBE.

RNA-seq and bioinformatics analysis

MrgprA3$^+$ and MrgprA3$^-$ neurons from every animal were collected and subjected to FACS. MrgprA3$^+$ neurons were collected based on GFP fluorescent. FACS gating for MrgprA3$^-$ cells was selected to collect cells that have similar morphological characteristics as the GFP$^+$ cells in

an effort to minimize contamination from other cell types such as satellite glial cells, Schwann cells, and endothelial cells whose sizes are much smaller than sensory neurons. RNA was isolated using the RNeasy Micro Kits (Qiagen). One ACD-A3$^+$ RNA sample was removed due to low RNA quality. Therefore, 5 Ctrl-A3$^+$, 5 Ctrl-A3$^-$, 4 ACD-A3$^+$, and 5 ACD-A3$^-$ RNA samples were used for RNAseq analysis. Library construction and RNA-seq were performed by BGI Genomics. Briefly, polyadenylated mRNA libraries were generated for cDNA library construction, amplification, and sequencing. RNA-seq was performed with the illumina HiSeq^{TM} 4000 at a depth of 50 million single-end reads of 50 bp. Clean reads are mapped to reference genome by Bowtie2 (Langmead and Salzberg, 2012), and then mapped read counts were normalized to the number of Fragments Per Kilobase of transcript per Million mapped reads (FPKM). FPKM levels for all genes in all samples are listed in Supplementary Table S5. We examined the expression levels of markers for non-neural cells in our results. We found that the expression of markers for Satellite glial cells (Gfap), endothelial cells (Emcn, Ecscr, and Cdh5), and Schwann cells (Mag and Pmp2) in all samples were very low (FPKM~0-0.2), suggesting that the possible contamination of non-neural cells is minimal.

Principal component analysis (PCA) was conducted using the FPKM data. To classify ACD and Ctrl conditions, we used support vector machine (svm) method (Cortes and Vapnik, 1995, Fawcett, 2006) to analyze the MrgprA3$^+$ and MrgprA3$^-$ samples, taking the top 11 PCs that explain 99% of the transcriptome profile variance. We used the DESeq2 tool (Love et al., 2014) to identify differentially expressed genes (DEGs). Criteria to identify DEGs in Ctrl-MrgprA3$^+$ vs Ctrl-MrgprA3$^-$ neurons comparison is FDR < 0.05 and fold change > 1.85. Criteria to identify DEGs in Ctrl-MrgprA3$^+$ vs ACD-MrgprA3$^+$ comparison is $p < 0.05$ and fold change > 1.3. All DEGs (totally 584) enriched in MrgprA3$^+$ neurons and top 700 DEGs enriched in MrgprA3$^-$

neurons were identified and subjected for gene ontology (GO) analysis using WEB-based GEne SeT AnaLysis Toolkit (WebGestalt). All DEGs (833 genes in MrgprA3$^+$ neurons and 712 genes in MrgprA3$^-$ neurons) in Ctrl-MrgprA3$^+$ vs AEW-MrgprA3$^-$ neurons comparison were used for ontology analysis. Heat-maps were generated using the normalized read counts per gene. To enhance the visibility of the heat-maps, the read counts were normalized by subtracting the median count per gene and divided by the median absolute deviation per gene.

In situ **hybridization**

Three 2-3 months old C57BL/6 mice were used for every double or triple *in situ* hybridization analysis. 6-8 lumbar ganglia were quickly collected from each mouse and frozen in dry-ice-cooled OCT medium. DRGs were sectioned at a thickness of 20 μm and *in situ* hybridization was performed using the RNAscope fluorescent multiplex kit (ACD Cat#320850) according to the manufacturer's instructions. The following probes were used: Mm-MrgprA3-C2 (Cat#: 548161-C2), Mm-Ptpn6-C1 (Cat#: 450081), Mm-Pcdh12-C1 (Cat#: 489891), Mm-Hrh1-C1 (Cat#: 491141), Mm-Hrh2-C1 (Cat#: 517751), Mm-Plcb3-C3 (Cat#:498071-C3). 7000-8000 sensory neurons (about 30-40 lumbar DRG sections) from each animal were counted to examine the percentage of DRG sensory neurons that are expressing each gene. Only cells containing nuclei labeled by DAPI were counted to avoid repetitive counting of the same cells in different sections.

Real-time RT-PCR

Real-time RT-PCR analysis were performed to examine the gene expression changes in allergic contact dermatitis model. The protocol to generate ACD model is describe in the "Mice and contact dermatitis" section. 5 mice were used in both control and SADBE group and dorsal root

ganglia (DRGs) innervating the treated skin area (T11-L6) were collected from every animal.

T12 DRG, which is immediately caudal to the last rib of the animal, was used as the landmark to

identify the axial level of all collected DRGs. Total RNA was extracted from the ganglia using

the RNeasy Micro Kits (Qiagen) according to the manufacturer's protocol. cDNA were

generated using SuperScript® III First-Strand Synthesis System (Invitrogen). Quantitative real-

time PCR was performed using a StepOnePlus Real-Time PCR System (Thermo Fisher

Scientific) with the SYBR Green detection method. The cycle threshold (C_T) values were

analyzed by the $2^{-\Delta Ct}$ method to determine the normalized expression ratio of target genes.

GAPDH expression level was used as the internal control. The intron-spanning primers used are

listed here: GAPDH Forward 5′-TGACCTCAACTACATGGTCTACA-3′, Reverse 5′-

CTTCCCATTCTCGGCCTT G-3′; Runx1 Forward 5'-CAAATCCGCCACAAGTTGCC-3',

Reverse 5'-GCCGCTCGGAAAAGGACAAA-3'; Il31ra Forward 5'-

GCCACGATCACATGGAAGGA-3', Reverse 5'- CACTGCAGGGCATGAGAGTT-3'; Kcne3

Forward 5'-ATCCGGGGACTCAAGGAAGA-3', Reverse 5'-

AGGAAAGGCCCAGAGCTAGA-3'; Syt7 Forward 5'-GTCACTATCGTCCTCTGCGG-3',

Reverse 5'-GACAGGAGCGTGCCATTGAG-3'; Camk2b Forward , Reverse; Dgkz Forward 5'-

GCACCTCAACTATGTGACGGA-3', Reverse 5'- TCTGGTCACGGTGCATGAG-3'.

DATA AVAILABILITY STATEMENT

We have deposited the related RNAseq data to GEO (Accession number is GSE146876).

AUTHOR CONTRIBUTION

Conceptualization: LH, JY; Formal Analysis: YX, JC, JY, LH; Investigation: YX, JC, HH, HS, JY, LH; Resources: HH; Writing - Original Draft Preparation: LH; Writing - Review and Editing: YX, JC, HH, HS, JY; Supervision: JY, LH; Funding Acquisition: JY, LH.

CONFLICT OF INTEREST

The authors claim no conflict of interest.

ACKNOWLEDGMENTS

REFERENCES

Azimi E, Reddy VB, Pereira PJS, Talbot S, Woolf CJ, Lerner EA. Substance P activates Mas-related G protein-coupled receptors to induce itch. J Allergy Clin Immunol 2017;140(2):447-53 e3.

Bacaj T, Wu D, Yang X, Morishita W, Zhou P, Xu W, et al. Synaptotagmin-1 and synaptotagmin-7 trigger synchronous and asynchronous phases of neurotransmitter release. Neuron 2013;80(4):947-59.

Bartesaghi L, Wang Y, Fontanet P, Wanderoy S, Berger F, Wu H, et al. PRDM12 Is Required for Initiation of the Nociceptive Neuron Lineage during Neurogenesis. Cell Rep 2019;26(13):3484-92 e4.

Basbaum AI, Bautista DM, Scherrer G, Julius D. Cellular and molecular mechanisms of pain. Cell 2009;139(2):267-84.

Chen CL, Broom DC, Liu Y, de Nooij JC, Li Z, Cen C, et al. Runx1 determines nociceptive sensory neuron phenotype and is required for thermal and neuropathic pain. Neuron 2006;49(3):365-77.

Chiu IM, Barrett LB, Williams EK, Strochlic DE, Lee S, Weyer AD, et al. Transcriptional profiling at whole population and single cell levels reveals somatosensory neuron molecular diversity. Elife 2014;3.

Cortes C, Vapnik V. Support-Vector Networks. Mach Learn 1995;20(3):273-97.

Desiderio S, Vermeiren S, Van Campenhout C, Kricha S, Malki E, Richts S, et al. Prdm12 Directs Nociceptive Sensory Neuron Development by Regulating the Expression of the NGF Receptor TrkA. Cell Rep 2019;26(13):3522-36 e5.

Di Marco E, Marchisio PC, Bondanza S, Franzi AT, Cancedda R, De Luca M. Growth-regulated synthesis and secretion of biologically active nerve growth factor by human keratinocytes. J Biol Chem 1991;266(32):21718-22.

Dou YC, Hagstromer L, Emtestam L, Johansson O. Increased nerve growth factor and its receptors in atopic dermatitis: an immunohistochemical study. Arch Dermatol Res 2006;298(1):31-7.

Emrick JJ, Mathur A, Wei J, Gracheva EO, Gronert K, Rosenblum MD, et al. Tissue-specific contributions of Tmem79 to atopic dermatitis and mast cell-mediated histaminergic itch. Proc Natl Acad Sci U S A 2018;115(51):E12091-E100.

Fawcett T. An introduction to ROC analysis. Pattern Recogn Lett 2006;27(8):861-74.

Fogh K, Herlin T, Kragballe K. Eicosanoids in skin of patients with atopic dermatitis: prostaglandin E2 and leukotriene B4 are present in biologically active concentrations. J Allergy Clin Immunol 1989;83(2 Pt 1):450-5.

Fontanet P, Irala D, Alsina FC, Paratcha G, Ledda F. Pea3 transcription factor family members Etv4 and Etv5 mediate retrograde signaling and axonal growth of DRG sensory neurons in response to NGF. J Neurosci 2013;33(40):15940-51.

Han L, Dong X. Itch mechanisms and circuits. Annu Rev Biophys 2014;43:331-55.

Han L, Ma C, Liu Q, Weng HJ, Cui Y, Tang Z, et al. A subpopulation of nociceptors specifically linked to itch. Nat Neurosci 2013;16(2):174-82.

Han SK, Mancino V, Simon MI. Phospholipase Cbeta 3 mediates the scratching response activated by the histamine H1 receptor on C-fiber nociceptive neurons. Neuron 2006;52(4):691-703.

Hu G, Huang K, Hu Y, Du G, Xue Z, Zhu X, et al. Single-cell RNA-seq reveals distinct injury responses in different types of DRG sensory neurons. Sci Rep 2016;6:31851.

Huang J, Polgar E, Solinski HJ, Mishra SK, Tseng PY, Iwagaki N, et al. Circuit dissection of the role of somatostatin in itch and pain. Nat Neurosci 2018;21(5):707-16.

Ikoma A, Steinhoff M, Stander S, Yosipovitch G, Schmelz M. The neurobiology of itch. Nat Rev Neurosci 2006;7(7):535-47.

Kido-Nakahara M, Buddenkotte J, Kempkes C, Ikoma A, Cevikbas F, Akiyama T, et al. Neural peptidase endothelin-converting enzyme 1 regulates endothelin 1-induced pruritus. J Clin Invest 2014;124(6):2683-95.

Konishi Y, Ikeda K, Iwakura Y, Kawakami K. Six1 and Six4 promote survival of sensory neurons during early trigeminal gangliogenesis. Brain Res 2006;1116(1):93-102.

Kramer I, Sigrist M, de Nooij JC, Taniuchi I, Jessell TM, Arber S. A role for Runx transcription factor signaling in dorsal root ganglion sensory neuron diversification. Neuron 2006;49(3):379-93.

Kremer AE, Martens JJ, Kulik W, Rueff F, Kuiper EM, van Buuren HR, et al. Lysophosphatidic acid is a potential mediator of cholestatic pruritus. Gastroenterology 2010;139(3):1008-18, 18 e1.

21

Kupari J, Haring M, Agirre E, Castelo-Branco G, Ernfors P. An Atlas of Vagal Sensory Neurons and Their Molecular Specialization. Cell Rep 2019;27(8):2508-23 e4.

Lallemend F, Ernfors P. Molecular interactions underlying the specification of sensory neurons. Trends Neurosci 2012;35(6):373-81.

Langmead B, Salzberg SL. Fast gapped-read alignment with Bowtie 2. Nat Methods 2012;9(4):357-U54.

Li CL, Li KC, Wu D, Chen Y, Luo H, Zhao JR, et al. Somatosensory neuron types identified by high-coverage single-cell RNA-sequencing and functional heterogeneity. Cell Res 2016;26(1):83-102.

Liu H, Bai H, Hui E, Yang L, Evans CS, Wang Z, et al. Synaptotagmin 7 functions as a Ca2+-sensor for synaptic vesicle replenishment. Elife 2014;3:e01524.

Liu Q, Sikand P, Ma C, Tang Z, Han L, Li Z, et al. Mechanisms of itch evoked by beta-alanine. J Neurosci 2012;32(42):14532-7.

Liu Q, Tang Z, Surdenikova L, Kim S, Patel KN, Kim A, et al. Sensory neuron-specific GPCR Mrgprs are itch receptors mediating chloroquine-induced pruritus. Cell 2009;139(7):1353-65.

Liu Q, Weng HJ, Patel KN, Tang Z, Bai H, Steinhoff M, et al. The distinct roles of two GPCRs, MrgprC11 and PAR2, in itch and hyperalgesia. Sci Signal 2011;4(181):ra45.

Liu Y, Yang FC, Okuda T, Dong X, Zylka MJ, Chen CL, et al. Mechanisms of compartmentalized expression of Mrg class G-protein-coupled sensory receptors. J Neurosci 2008;28(1):125-32.

Lou S, Pan X, Huang T, Duan B, Yang FC, Yang J, et al. Incoherent feed-forward regulatory loops control segregation of C-mechanoreceptors, nociceptors, and pruriceptors. J Neurosci 2015;35(13):5317-29.

Love MI, Huber W, Anders S. Moderated estimation of fold change and dispersion for RNA-seq data with DESeq2. Genome Biol 2014;15(12):550.

Meixiong J, Dong X. Mas-Related G Protein-Coupled Receptors and the Biology of Itch Sensation. Annu Rev Genet 2017;51:103-21.

Meixiong J, Vasavda C, Green D, Zheng Q, Qi L, Kwatra SG, et al. Identification of a bilirubin receptor that may mediate a component of cholestatic itch. Elife 2019a;8.

Meixiong J, Vasavda C, Snyder SH, Dong X. MRGPRX4 is a G protein-coupled receptor activated by bile acids that may contribute to cholestatic pruritus. Proc Natl Acad Sci U S A 2019b;116(21):10525-30.

Mishra SK, Hoon MA. The cells and circuitry for itch responses in mice. Science 2013;340(6135):968-71.

Mollanazar NK, Smith PK, Yosipovitch G. Mediators of Chronic Pruritus in Atopic Dermatitis: Getting the Itch Out? Clin Rev Allergy Immunol 2016;51(3):263-92.

Moody SA, LaMantia AS. Transcriptional regulation of cranial sensory placode development. Curr Top Dev Biol 2015;111:301-50.

Morita T, McClain SP, Batia LM, Pellegrino M, Wilson SR, Kienzler MA, et al. HTR7 Mediates Serotonergic Acute and Chronic Itch. Neuron 2015;87(1):124-38.

Patel TD, Jackman A, Rice FL, Kucera J, Snider WD. Development of sensory neurons in the absence of NGF/TrkA signaling in vivo. Neuron 2000;25(2):345-57.

Piomelli D, Sasso O. Peripheral gating of pain signals by endogenous lipid mediators. Nat Neurosci 2014;17(2):164-74.

Qu L, Fan N, Ma C, Wang T, Han L, Fu K, et al. Enhanced excitability of MRGPRA3- and MRGPRD-positive nociceptors in a model of inflammatory itch and pain. Brain 2014;137(Pt 4):1039-50.

Reddy VB, Lerner EA. Activation of mas-related G-protein-coupled receptors by the house dust mite cysteine protease Der p1 provides a new mechanism linking allergy and inflammation. J Biol Chem 2017;292(42):17399-406.

Reddy VB, Sun S, Azimi E, Elmariah SB, Dong X, Lerner EA. Redefining the concept of protease-activated receptors: cathepsin S evokes itch via activation of Mrgprs. Nat Commun 2015;6:7864.

Salvatierra J, Diaz-Bustamante M, Meixiong J, Tierney E, Dong X, Bosmans F. A disease mutation reveals a role for NaV1.9 in acute itch. J Clin Invest 2018;128(12):5434-47.

Sano Y, Inamura K, Miyake A, Mochizuki S, Kitada C, Yokoi H, et al. A novel two-pore domain K+ channel, TRESK, is localized in the spinal cord. J Biol Chem 2003;278(30):27406-12.

Secundo L, Snitz K, Sobel N. The perceptual logic of smell. Curr Opin Neurobiol 2014;25:107-15.

Sharma N, Flaherty K, Lezgiyeva K, Wagner DE, Klein AM, Ginty DD. The emergence of transcriptional identity in somatosensory neurons. Nature 2020;577(7790):392-8.

Shirai Y, Saito N. Diacylglycerol kinase as a possible therapeutic target for neuronal diseases. J Biomed Sci 2014;21:28.

Solinski HJ, Kriegbaum MC, Tseng PY, Earnest TW, Gu X, Barik A, et al. Nppb Neurons Are Sensors of Mast Cell-Induced Itch. Cell Rep 2019;26(13):3561-73 e4.

Storan ER, O'Gorman SM, McDonald ID, Steinhoff M. Role of cytokines and chemokines in itch. Handb Exp Pharmacol 2015;226:163-76.

Suzuki M. The Drosophila tweety family: molecular candidates for large-conductance Ca2+-activated Cl- channels. Exp Physiol 2006;91(1):141-7.

Tominaga M, Tengara S, Kamo A, Ogawa H, Takamori K. Matrix metalloproteinase-8 is involved in dermal nerve growth: implications for possible application to pruritus from in vitro models. J Invest Dermatol 2011;131(10):2105-12.

Usoskin D, Furlan A, Islam S, Abdo H, Lonnerberg P, Lou D, et al. Unbiased classification of sensory neuron types by large-scale single-cell RNA sequencing. Nat Neurosci 2015;18(1):145-53.

Wan L, Jin H, Liu XY, Jeffry J, Barry DM, Shen KF, et al. Distinct roles of NMB and GRP in itch transmission. Sci Rep 2017;7(1):15466.

Waxman SG, Zamponi GW. Regulating excitability of peripheral afferents: emerging ion channel targets. Nat Neurosci 2014;17(2):153-63.

Yajima H, Suzuki M, Ochi H, Ikeda K, Sato S, Yamamura K, et al. Six1 is a key regulator of the developmental and evolutionary architecture of sensory neurons in craniates. BMC Biol 2014;12:40.

Yarmolinsky DA, Zuker CS, Ryba NJ. Common sense about taste: from mammals to insects. Cell 2009;139(2):234-44.

Yosipovitch G, Bernhard JD. Clinical practice. Chronic pruritus. The New England journal of medicine 2013;368(17):1625-34.

Yu H, Zhao T, Liu S, Wu Q, Johnson O, Wu Z, et al. MRGPRX4 is a bile acid receptor for human cholestatic itch. Elife 2019;8.

Zeisel A, Hochgerner H, Lonnerberg P, Johnsson A, Memic F, van der Zwan J, et al. Molecular Architecture of the Mouse Nervous System. Cell 2018;174(4):999-1014 e22.

Zhu Y, Hanson CE, Liu Q, Han L. Mrgprs activation is required for chronic itch conditions in mice. Itch (Phila) 2017;2(3).

FIGURE LEGENDS

Figure 1. MrgprA3$^+$ neurons are distinct itch-sensing neurons.

(A) Hematoxylin and eosin (H&E) staining of the skin sections collected from *MrgprA3$^{GFP-Cre}$*
mice after SADBE or vehicle control treatments. SADBE induced contact dermatitis in the skin
evidenced by the parakeratosis and inflammatory cells infiltration in the skin. (B) *MrgprA3^{GFP-}*
^{Cre} mice developed robust scratching behavior after the allergic contact dermatitis treatment. N =
5 mice for each group. (C) Principal component analysis shows distinct transcriptome
segregation of MrgprA3$^+$ neurons and MrgprA3$^-$ neurons. (D) Control and ACD conditions were
classified with SVM-based classification model. The area under the ROC curve (AUC) is clearly
higher for the MrgprA3$^+$ neuron samples compare to MrgprA3$^-$ neurons. (E-F) Gene ontology
(GO) Biological Process (E) and Molecular Function (F) categories analysis of enriched genes in
MrgprA3$^+$ and MrgprA3$^-$ neurons. All -log$_{10}$(P) >15 was defined as 15 to fit the graph. ***$P <$
0.005. Two-tailed unpaired Student's t-test. Error bars represent s.e.m. Scale bar = 100 μm.

**Figure 2. Heat-maps showing the expression pattern of sensory neuron markers in
MrgprA3$^+$ and MrgprA3$^-$ neurons.**

Differentially expressed Mrgprs (A), itch-related molecules (B), TRP channels (C), nociception-
related molecules (D), neurotrophin receptors (E), other sensory neuron markers (F), and
neuropeptides (G) were analyzed and plotted in heat-maps. Columns are individual samples.

Figure 3. Heat-maps showing the expression pattern of ion channels.

Differentially expressed sodium channels (A), calcium channels (B), chloride channels (C), and
potassium channels (D) were analyzed and plotted in heat-maps. Columns are individual samples.

Figure 4. *In situ* hybridization validation of identified markers in MrgprA3⁺ neurons.

(A-B) Fluorescent *in situ* hybridization and Venn diagrams showing the expression overlapping of Hrh1 (A), Hrh2 (B), PLCβ3 (A-B), Ptpn6 (C), and Pcdh12 (D) with MrgprA3. Scale bar = 20 μm.

Figure 5. MrgprA3⁺ and MrgprA3⁻ neurons are differentially affected by the allergic contact dermatitis condition.

(A) Venn diagram showing the minimal overlap of genes changed by ACD condition in MrgprA3⁺ and MrgprA3⁻ neurons. Numbers inside of the circle indicate the number of genes identified in the analysis. A3: MrgprA3⁺ neurons, N: MrgprA3⁻ neurons, ACD: allergic contact dermatitis. (B) Gene ontology analysis of genes changed by the ACD treatment.

Figure 6. Heat-maps showing transcripts changed by ACD treatment in MrgprA3⁺ and MrgprA3⁻ neurons.

Lists of transcription factors (A), nociception-related genes (B), ion channels (C), neurotransmitter receptors (D), synapse-related genes (E) whose expression were changed by the ACD treatment in MrgprA3⁺ and MrgprA3⁻ neurons. For genes that were not significantly changed by ACD ($p > 0.05$), the value of $\log_2$(Foldchange) was defined as 0. (F) Real-time PCR results showing the expression changes of six representative genes after ACD treatment. $n = 5$ mice for each group. $*P < 0.05$, $**P < 0.01$, $***P < 0.005$. Two-tailed unpaired Student's t-test. Error bars represent s.e.m.

Supplementary Table 1: Differentially expressed genes in MrgprA3⁺ neurons compared to MrgprA3⁻ neurons under naïve condition.

25

Supplementary Table 2: List of genes that were significantly changed by ACD in MrgprA3$^+$ neurons.

Supplementary Table 3: List of genes that were significantly changed by ACD in MrgprA3$^-$ neurons.

Supplementary Table 4: List of genes whose expression were changed by ACD in both MrgprA3$^+$ and MrgprA3$^-$ neurons.

Supplementary Table 5: FKPM values of all genes in all samples.

a

Control

ACD

b

Scratching bouts

100
80
60
40
20
0

***

Ctrl   ACD

c

Principal Component Analysis

PC2

2000
1000
0
-1000
-2000
-3000

-4000   0   4000

PC1

● Ctrl-A3+
● Ctrl-A3-
■ ACD-A3+
■ ACD-A3-

d

True Positive Percentage

100
80
60
40
20
0

0 20 40 60 80 100

False Positive Percentage

AUC: 100%
AUC: 52%

— MrgprA3+
— MrgprA3-

e

GO Biological Process

MrgprA3+

GO:0022008 Neurogenesis
GO:0030182 Neuron differentiation
GO:0006811 Ion transport
GO:0051592 Response to calcium ion
GO:0033198 Response to ATP
GO:0060081 Membrane hyperpolarization
Custom Itch

MrgprA3-

GO:0022008 Neurogenesis
GO:0030182 Neuron differentiation
GO:0006811 Ion transport
GO:0007268 Synaptic transmission
GO:0001508 Action potential
GO:0040011 Locomotion
GO:0050954 Mechanical sensation
GO:0019233 Pain
GO:0009266 Thermal sensation

15   10   5   0   5

$-\log_{10}(P)$

f

GO Molecular Function

MrgprA3+

GO:0022857 Transmembrane transporter
GO:0005261 Cation channel
GO:0005030 Neurotrophin receptor
GO:0005227 Calcium-activated cation channel

MrgprA3-

GO:0022857 Transmembrane transporter
GO:0005261 Cation channel
GO:0030594 Neurotransmitter receptor
GO:0008188 Neuropeptide receptor
GO:0019838 Growth factor binding
GO:0019955 Cytokine binding
GO:0005267 Potassium channel

15   10   5   0   5

$-\log_{10}(P)$

a   Mrgprs

MrgprA3⁺   MrgprA3⁻

Mrgprb4
Mrgpra8
Mrgpra7
Mrgpra4
Mrgpra3
Mrgprc11
Mrgpra2b
Mrgpra1
Mrgprd

b   Itch-related molecules

MrgprA3⁺   MrgprA3⁻

Hrh2
Hrh1
Nmb
Plcb3
Ednrb
Cysltr2
S1pr3
Tlr3
Nppb
Htr7
Sst
Lpar1
Htr1f
Tlr4
Lpar3
Il31ra
Crlf2
Ece1
S1pr1

c   TRP channels

MrgprA3⁺   MrgprA3⁻

Trpc3
Trpm8
Trpm2
Trpv1
Trpa1
Trpv2

d   Nociception-related
molecules

MrgprA3⁺   MrgprA3⁻

P2ry2
P2rx2
Ptger4
Ptgfr
Asic1
P2ry1
Asic3
Ano1
Ptgr2
Ptgr1

e   Neurotrophin receptors

MrgprA3⁺   MrgprA3⁻

Gfra1
Runx2
Ntrk1
Ret
Ntrk3
Runx3
Runx1
Ntrk2
Gfra3
Gfra2

f   Other sensory neuron markers

MrgprA3⁺   MrgprA3⁻

Prdm12
Ina
Slc17a7 (vGlut1)
Piezo1
Piezo2
Cacna1h
Spp1
Nefh
Fam19a1
Slc17a8 (vGlut3)
Th
Ldhb
Pvalb
Nefm
Slc17a6(vGlut2)

g   Neuropeptides

MrgprA3⁺   MrgprA3⁻

Agrp
Pcsk2
Calca
Calcb
Pcsk1n
Gal
Tac1
Cartpt
Nts
Adcyap1
Scg2
Chgb
Pcsk9

min   max
FPKM

a

Sodium Channels

	MrgprA3+					MrgprA3-				
Scn3b										
Scn2b										
Scn11a (Nav1.9)										
Scn10a (Nav1.8)										
Scn9a (Nav1.7)										
Scn8a										
Scn3a										
Scn1a										
Scn4b										
Scn5a										
Scn7a										
Scn4a										
Scn2a1										

b

Calcium Channels

	MrgprA3+					MrgprA3-				
Cacng2										
Cacnb3										
Cacna1b										
Cacna1h										
Cacng5										
Cacnag3										
Cacn1d										
Cacnb4										

c

Chloride Channels

	MrgprA3+					MrgprA3-				
Ttyh2										
Ttyh3										
Ano1										
Clcn5										
Clcn6										

d

Potassium Channels

	MrgprA3+					MrgprA3-				
Kcnn2										
Kcnk18										
Kcna5										
Kcnj11										
Kctd8										
Kcnj12										
Kcnt1										
Kcnmb1										
Kctd17										
Kcnc4										
Kcns1										
Kctd15										
Kcnh8										
Kcnh1										
Kcnc1										
Kcnt2										
Kcnh2										
Kcnf1										
Kcnq5										
Kcnh7										
Kcnk2										
Kcnk3										
Kcna1										
Kcna2										
Kcnmb2										
Kcnk1										
Kcnma1										
Kcna4										
Kcnc2										
Kcnip1										
Kcnab1										

min ▬ max
FPKM

a   MrgprA3   Hrh1   PLCβ3   Merge/DAPI

Hrh1/Hrh2   MrgprA3

PLCβ3

$$\frac{Hrh1+PLCβ3}{MrgprA3} = 82.9\%$$

$$\frac{Hrh2+PLCβ3}{MrgprA3} = 84.9\%$$

b   MrgprA3   Hrh2   PLCβ3   Merge/DAPI

c   MrgprA3   Ptpn6   Merge/DAPI

Ptpn6   MrgprA3

$$\frac{MrgprA3}{Ptpn6} = 83.3\%$$

$$\frac{Ptpn6}{MrgprA3} = 47.1\%$$

d   MrgprA3   Pcdh12   Merge/DAPI

Pcdh12   MrgprA3

$$\frac{MrgprA3}{Pcdh12} = 69.9\%$$

$$\frac{Pcdh12}{MrgprA3} = 75\%$$

a

b

GO Biological Process

GO:0012501 Programmed cell death
GO:0033554 Cellular response to stress
GO:0051276 Chromosome organization
GO:0016570 Histone modification
GO:0022008 Neurogenesis
GO:0097484 Dendrite extension
GO:0007010 Cytoskeleton organization
GO:0046907 Intracellular transport

GO:0006974 Cellular response to DNA damage
GO:0009894 Regulation of catabolic process
GO:0016311 Dephosphorylation
GO:0048193 Golgi vesicle transport

GO:0007268 Chemical synaptic transmission
GO:0098655 Cation transmembrane transport
GO:0000165 MAPK cascade
GO:0007264 Small GTPase signal transduction
GO:0051090 Transcription factor activity